Rare Gas Mobility in Pure and Doped Potassium Bromide

HJ. MATZKE *

Institut für Kern- und Radiochemie der Technischen Hochschule Braunschweig, Germany

(Z. Naturforschg. **22 a**, 507—518 [1967]; received 25 November 1966)

The mobility of the inert gases argon and xenon in pure and doped single crystals of KBr was studied. The gases were introduced by ion bombardment. The recently established system of stages was used to interpret the results. Normal volume diffusion was found for xenon at low gas concentration, the activation enthalpy being 1.4 ± 0.2 eV. This release was independent of doping, thus favoring a transport process for xenon independent of single vacancies. As most probable alternative, a mobility via small vacancy clusters, e. g. vacancy pairs was suggested. Trapping of xenon was found at higher xenon concentrations. This retarded release was shown to depend on doping and was more pronounced in crystals with an excess of cation vacancies. The diffusion of argon occurred with a similar activation enthalpy, but was most probably due to an interstitial motion.

The diffusion of rare gases from KBr and its mechanism are of interest because KBr can be regarded as a "model substance" for nuclear fuel materials with a similar lattice structure (e. g. UC, UN). Furthermore, diffusion constants in potassium bearing minerals are frequently needed for determinations of geological ages to correct for diffusional losses of rare gases [1].

Ion bombardment has been shown to be a valuable tool in gas release work on various ionic crystals and sinters [2–4]. The possibility of achieving greatly different gas concentrations and varying penetration depths provides an easy means of studying the effects of damage, gas concentration and surface proximity.

To study the mechanism of rare gas diffusion, doped materials were used in the cases of xenon diffusion in UO_2 [2] and ThO_2 [5], and argon diffusion in CaF_2 [6, 7]. For all these materials a clear picture of the lattice disorder exists. This enables one to predict the effects of doping on lattice disorder and self-diffusion. Thus, a possible influence of self-diffusion or specific vacancies on gas release can be studied. Very little, if any, influence of doping on gas release was found at low gas concentrations. Thus, a mechanism for rare-gas diffusion independent of self-diffusion was favoured. At high gas concentrations, however, gas release was found to depend on doping in all three substances UO_2, ThO_2 and CaF_2 though still without implying a mechanism similar to self-diffusion [2, 5, 7].

KBr is known to have the SCHOTTKY type of disorder, i. e. the prevailing defects are potassium and bromine vacancies in equal concentrations. By adding suitable divalent impurities, the concentration of one kind of vacancy can be increased and that of the other decreased in proportion. The basic mobility data for the lattice ions have been reported by ROLFE [8]. By comparing release data obtained on pure single crystals with those obtained on crystals doped with positive and negative divalent impurities it was hoped to improve the understanding of the basic transport processes for rare gases.

The recently established system of stages [4, 9], which will be described in Section 2, was mainly used in the interpretation. Thus, most results were obtained by using isochronal heatings at about 100 °C intervals, because it was found that this type of experiment resolves coexisting transport processes more clearly than do alternatives such as isothermal heatings. When the samples are heated isochronally each process tends to go to completion separately. Most results were therefore presented as plots of the fractional release of gas, F, versus temperature, T. By varying the gas concentration and using a suitable bombardment energy, the stages could be studied separately.

* This work was done during a Post-Doctoral Fellowship of the National Research Council, Ottawa, while the author was attached to the Chemistry and Metallurgy Division of Atomic Energy of Canada Limited, Chalk River, Ontario.

[1] W. GENTNER and W. KLEY, Z. Naturforschg. **10 a**, 832 [1955].
[2] HJ. MATZKE, Nucl. Appl. **2**, 131 [1966].
[3] HJ. MATZKE and J. L. WHITTON, Can. J. Phys. **44**, 995 [1966].
[4] R. KELLY and HJ. MATZKE, J. Nucl. Mater. **17**, 179 [1965].
[5] HJ. MATZKE, J. Nucl. Mater. **21**, 190 [1967].
[6] T. LAGERWALL, Nukleonik **6**, 179 [1964].
[7] HJ. MATZKE, Z. Naturforschg., to be published.
[8] J. ROLFE, Can. J. Phys. **42**, 2195 [1964].
[9] R. KELLY and F. BROWN, Acta Met. **13**, 169 [1965].

1. Materials

Single crystals of pure and doped KBr, grown from the melt using a vertical-pull cooled-seed method, were obtained from Dr. J. ROLFE (NRC, Ottawa). Specimens for gas release studies were cleaved discs about 1 to 2 mm thick, and about 1 cm square. The pure crystals had residual concentrations of divalent impurities of about 0.01 ppm, corresponding to a "knee-temperature" for electrical conductivity (onset of intrinsic behaviour) of about 360 °C. This concentration is negligible compared to the addition of impurities in the doped crystals: 200 ppm K_2CO_3 and 500 ppm $CaBr_2$, respectively. These values have to be compared with the number of SCHOTTKY defects in thermal equilibrium which is at the melting point about 30 ppm [8]. However, for a significant comparison one has to verify that all the impurities are in solid solution and no associations of impurities and vacancies occur.

In the temperature range used in this work, i. e. 50 to 600 °C, most of the K_2CO_3 will be insoluble. The solubility at 600 °C is about 50 ppm, at 400 °C roughly 1 ppm [8]. $CaBr_2$, on the other hand, is more soluble in KBr, the solubility being roughly 10 ppm at 200 °C and roughly 700 ppm at 600 °C. Thus, K_2CO_3 will only be effective at relatively high temperatures ($\geqq$ 500 °C) whereas $CaBr_2$ should be effective at all experimental temperatures.

Besides single crystals, evaporated KBr layers of various thickness were used in some experiments. These layers did not show any indication of crystallinity in reflection electron diffraction pattern. This indicated either amorphousness or microcrystallinity with extremely small grain size.

2. Kinetics of Gas-Release Following Ion-Bombardment

Early experiments on gas release from ceramics and ionic crystals have mostly been done using the emanation technique, or homogeneous labeling by nuclear reaction during reactor irradiation. Recently, recoil and ion-bombardment techniques have been used to introduce the gas into various solids. Which technique is chosen depends on what one wants to emphasize. By varying gas concentration and incident energy in ion bombardment work one is enabled to separate different release processes which otherwise might occur simultaneously leading to a release behaviour which is difficult to interpret and to analyze.

2.1. The system of stages

Ion bombardment experiments have led to the establishment of a system of stages for inert gas motion [4, 9, **], i. e. the observation of the general occurrence of three diffusion processes or stages. These occur at different temperatures or different temperature regions (see Fig. 1).

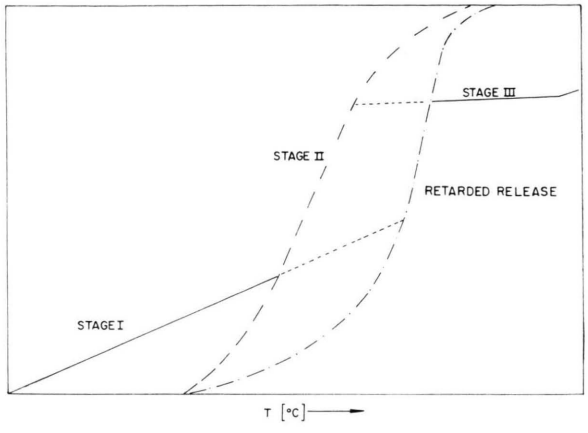

Fig. 1. The system of stages in a plot of F-versus-T.

Stage II represents normal, homogeneous volume diffusion and occurs often at temperatures compatible with self-diffusion. The dependence of the release on annealing time and geometry (or particle size) is therefore that given by FICK's law. Since the diffusion coefficient is a simple exponential function of temperature the curve of fractional release against temperature of isochronal anneals has a sigmoidal shape. For most materials, normal gas diffusion becomes appreciable at a temperature about half the melting point on the absolute scale. In some experiments, an increase in gas concentration leads to a shift of the sigmoidal release curve to higher temperatures indicating a "retarded release" (Fig. 1). In this case temporary or weak trapping of gas at

** The designation of stages originates from work on the recovery of physical changes introduced by irradiation, cold-working, and quenching. In most cases recovery of electrical resistivity has been studied. Qualitative similarities in the recovery behaviour are found which suggest that the various treatments show common recovery processes. Isochronal annealing is used to separate stages and isothermal curves show saturation levels corresponding to the isochronal structure. Differentiation of the isochronal recovery curves gives annealing peaks or substages each of which implies a separate recovery process. These substages are attributed to different mass transport processes. In the case of copper [10] five stages I ... V are generally accepted. These overlap partly in temperature, for the temperature intervals may be as small as 50 to 100 °K.

[10] J. W. CORBETT, R. B. SMITH, and R. M. WALKER, Phys. Rev. **114**, 152 and 1460 [1959].

bombardment induced defects, e. g. dislocation loops, probably occurs.

Stage I describes *any* release occuring at temperatures well below those for stage II. Stage I would therefore include diffusion along boundaries or diffusion pipes, release during phase transformations, release due to excess point defects etc. In the present context, however, the stage I release often exhibits specific kinetics: the fractional release is proportional to the logarithm of the annealing time in isothermal anneals and is proportional to the temperature in isochronal anneals, i. e. the isochronal plot is a straight line. KELLY [11] has shown that such kinetics can represent a process having a spectrum of activation enthalpies all lower than that for volume diffusion. Although stage I has been called "damage diffusion" it may equally well be associated with surface effects rather than with radiation damage. Stage I is discussed further by MATZKE and WHITTON [3] and JECH and KELLY [12].

Stage III describes release well above the high temperature end of the stage II range. Stage III is attributed to a strong trapping of the inert gas by pores, bubbles or other similar defects. This stage is discussed further by MACEWAN and MOREL [13] for the case of UO_2 and by RUEDL and KELLY [14] who connected stage III for the system krypton – platinum with the formation and movement of gas filled bubbles.

2.2. *Kinetics of stage II gas release following ion bombardment*

The distribution curve of the gas in a solid following ion bombardment depends, as the range does, on the nature and structure of the solid and on the nature and concentration of the gas used [15]. Actual range curves for KBr are given elsewhere [16]. They show that, for the bombardment conditions chosen, an exponential distribution is a fair approximation, while the following argument proves that small departures from the ideal distribution have little effect.

Fractional release expressions are available for the following distributions:

plane source [11]

$$F = \operatorname{erfc}(1/2\,x)\,; \qquad (1)$$

peaked distribution with exponential tail [4]

$$F = 1 - 2\,x/\sqrt{\pi} - (1 - 2\,x^2)\,\exp(x^2)\,\operatorname{erfc}(x)\,; \qquad (2)$$

exponential distribution [9]

$$F = 1 - \exp(0.480\,x^2)\,\operatorname{erfc}(\sqrt{0.480}\,x)\,; \qquad (3)$$

rectangular distribution [17]

$$F \approx 2\,x/\sqrt{\pi}\,\{1 - \exp(-1/4\,x^2)\} + \operatorname{erfc}(1/2\,x)\,; \qquad (4)$$

linearly decreasing distribution [17]

$$F \approx 1 - \{(2\,x^2 + 1)\,\operatorname{erfc}(1/2\,x) + 2\,x/\sqrt{\pi} \cdot [\exp(-1/4\,x^2) - 2)]\}\,. \qquad (5)$$

x^2 stands for $D\,t/R^2$, where R is the range of the gas which is the limit of penetration in the cases of a plane source, a rectangular and a linearly decreasing concentration profile. In the case of Eq. (2), the most probable or peak range R_p has to be used, while with Eq. (3) the median or 50% range R_m is used ($R_m \approx 1.68\,R_p$).

The functions (1) to (5) have been calculated and the results are plotted in Fig. 2. For easier presentation, all ranges have been transformed to R_m. In most cases, the actual distribution will be in between these idealized cases. Moreover, at the energy-dose combinations used in this work, it is reason-

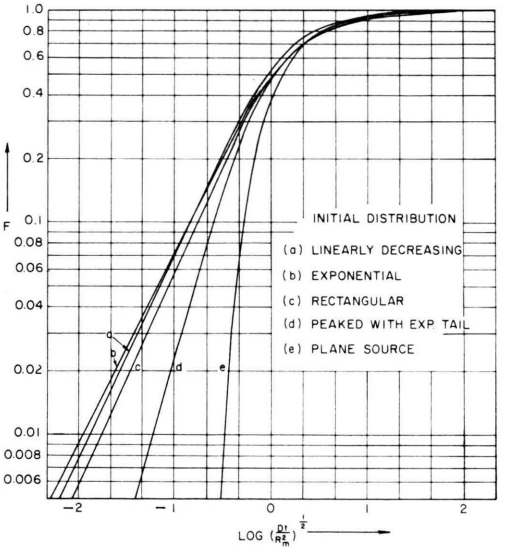

Fig. 2. Theoretical fractional release curves for different initial gases distributions [Eqs. (1) to (5)].

[11] R. KELLY, Can. J. Chem. **39**, 664 and 2411 [1961].
[12] C. JECH and R. KELLY, J. Nucl. Mater. **20**, 269 [1966].
[13] J. R. MACEWAN and P. MOREL, Nucl. Appl. **2**, 158 [1966].
[14] E. RUEDL and R. KELLY, J. Nucl. Mater. **16**, 89 [1965].
[15] R. KELLY and HJ. MATZKE, J. Nucl. Mater. **20**, 171 [1966].
[16] J. L. WHITTON and HJ. MATZKE, Can. J. Phys. **44**, 2905 [1966].
[17] G. DI COLA and HJ. MATZKE, Euratom Report EUR 2157.e [1964].

able to exclude the extreme case of a plane source as being a poor approximation ***. The four remaining cases yield similar release curves between $F = 0.2$ to $F = 0.8$, the actual differences in $(D\,t/R_m^2)^{1/2}$ being less than a factor of 1.4 (thus less than a factor of 2 in the diffusion coefficient D).

The five release curves of Fig. 2 are easily seen to be consistent with the geometries. With an exponential or a linearly decreasing distribution, most of the gas is close to the surface. Thus, given that D and R_m are constant, most release occurs at small values of t. With a peaked distribution and especially with a plane source, the gas is deeper in the solid. Hence the release starts at much bigger values of t. On the other hand, the exponential distribution contains some gas very deep in the solid; thus the high values of F are not reached before very high values of t.

2.3. Approaches to evaluate release curves of the type F-versus-T for stage II

A) At first approach to evaluating release curves of the F-versus-T type was made by KELLY and BROWN [9]. They assumed an idealized value of the pre-exponential factor D_0 and derived expressions for the activation enthalpy, ΔH, which contained the temperature, T, for a given fractional release, F, as the only variable. This method was extended by KELLY and MATZKE [4, 15] who gave relations for $F = 0.1$, 0.5, and 0.9 for various distributions and geometries. The general form of these relations is

$$\Delta H/T = (A \pm 5) - 4.6 \log R_m^2/t; \qquad (6)$$

where ΔH is in cal/mole, R_m is in units of atom layers, t is the annealing time at a given temperature in minutes and A is a constant which depends on the geometry and F-value; the uncertainity ± 5 arises from the assumptions about D_0 ($= 3 \times 10^{-1 \pm 1}$ cm^2 sec^{-1}; this range of values agrees best with the diffusion literature [4]). The different values for A are given in Table 1. Again it follows that the values obtained for ΔH differ only slightly for various geometries and shapes of the distribution curve.

In the following some other approaches are given.

B) One starts again from the basic ARRHENIUS equation

$$D = D_0 \exp(-\Delta H/R\,T). \qquad (7)$$

*** The plane source approximation may be useful for high dose, low energy bombardment when the penetration is comparable to the separation of lattice planes, or at very high energies [15].

Values A in Eq. (6).

Distribution	$F = 0.1$	$F = 0.5$	$F = 0.9$
exponential	83.3	75.0	67.2
peaked with tail	80.9	75.2	67.9
rectangular	86.8	78.5	70.7
linearly decreasing	91.2	83.7	75.9
plane source	78.8	75.2	68.5

Values B and C in Eqs. (8) and (9).

Distribution	$F = 0.2/0.5$		$F = 0.5/0.8$		$F = 0.2/0.8$	
	B	C	B	C	B	C
exponential	1.12	−0.50	1.14	0.63	2.26	0.07
peaked with tail	0.84	−0.35	1.00	0.55	1.84	0.14
rectangular	0.84	−0.50	0.94	0.39	1.78	−0.03
linearly decreasing	0.96	−0.51	0.98	0.41	1.94	−0.10
plane source	0.58	−0.05	0.82	0.65	1.40	0.36

Table 1. Constants for the diffusion Eqs. (6), (8), and (9).

By choosing two suitable values of the fractional release, F_1, F_2, and the corresponding temperatures, T_1, T_2, from the measured release curve and substituting the corresponding values of $D\,t/R_m^2$ from Fig. 2 one gets two equations. By division one obtains a value of ΔH independent of D_0, R_m, and t:

$$\Delta H = 4.6\,B\,T_1\,T_2/(T_2 - T_1)\ \text{kcal/mole}; \qquad (8)$$

B is a constant which depends on the choice of F_1 and F_2 and the distribution of the gas. This constant is given in Table 1 for the five distributions of Fig. 2 and the intervals $F = 0.2/0.5$, $0.5/0.8$ and $0.2/0.8$. By using this approach one has to make sure that the low values of F are not perturbed by stage I release (hence the choice of $F = 0.2$ rather than $F = 0.1$) and that the high values of F are not influenced by "retarded release" or stage III behaviour (hence the choice of $F = 0.8$ rather than $F = 0.9$). If agreement is achieved this approach gives a valuable confirmation of the ΔH value obtained from the first approach of a fixed D_0. Where stages I, III or "retarded release" give large contributions, the analysis of stage II is best made with approach A.

In case of disagreement in ΔH an approach can be used which does not assume a value for D_0, provided the range R is known or can be estimated. Using the above ΔH value and appropriate pairs of F_1, F_2 and hence T_1, T_2, one gets D_0 from an equation derived in a similar way to Eq. (8):

$$\log D_0 = 0.11\,\Delta H\,(T_1 + T_2)/T_1\,T_2 + \log R^2/t + C; \qquad (9)$$

Again, C is a constant depending on distribution and choice of F_1, F_2 (see Table 1), R is in units of

cm, t is the experimental annealing time in seconds. By using different pairs of F_1, F_2 a confirmation of the values is obtained.

C) Finally, one might read the corresponding D-values to each F-value, using Fig. 2, and get both ΔH and D_0 by plotting these data into an ARRHENIUS diagram. By using this method the experimental errors can easily be obtained by a least square fit.

All these methods have been used to evaluate the present results.

2.4. Integral depth distributions

For analyzing integral depth distributions, the only available solutions of the diffusion equation are for the two limiting cases of absence of trapping of gas and presence of *permanent* traps [15]. For these calculations it was assumed that at the beginning of the diffusion anneal no gas was trapped though the more general case of initial trapping differs only in an additive constant. No expressions have been published yet for the case of *weak* trapping, i. e. *temporary* interaction of gas and bombardment induced defects.

3. Experimental

3.1 Labeling of the specimens with rare gas using ion bombardment

The Chalk River electromagnetic mass separator was used to inject argon and xenon into the targets. The bombardment energy was varied between 0.5 and 40 keV. The bombardment time was always 10 to 30 min. The ion current incident on the specimen surface and hence the gas concentration could be varied by using different nuclides. Assuming that the main contribution to the beams of radio-active nuclides is a 0.1% overlap from the beams of the adjacent stable nuclides [18] and that the bombarded area is ≈ 1 cm², specific gas concentrations (given in terms of integrated current and in terms of number of incident ions/cm²) were obtained (see Table 2).

Nuclide	Total Current Used μAmin/cm²	Ion Current μAmin/cm²	Total Incident Ions/cm²
Xe-125	100	2×10^{-4}	8×10^{10}
Xe-133	300	0.1	4×10^{13}
Xe-131 + 133	200	~ 1	$\sim 4 \times 10^{14}$
Xe-131	200	44	2×10^{16}
Ar-41	200	0.2	8×10^{13}

Table 2. Gas concentrations used in mass-separator bombardments. — 1 μAmin/cm² = 4×10^{14} ions/cm². No allowance for sputtering and emission of secondary electrons is made.

Bombardment with xenon: Three main doses, each differing by a factor of about 500 from the next one, were obtained using the three isotopes Xe-125, Xe-133, and Xe-131 + 131^m. In some cases an intermediate dose was obtained by deflecting the beam alternatively to the Xe-131 and Xe-133 positions.

Bombardment with argon: By reactor irradiating natural argon, only Ar-41 is formed in high enough specific activity to be used in ion bombardment work. Thus, only this isotope could be employed despite its favourable short half-life of 1.82 h. Therefore, the integrated ion dose could not be varied considerably. A low dose could not be achieved because of the 0.1% overlapping of the beam of Ar-40 which has a high natural abundance.

All the nuclides used are radioactive except Xe-131. In this case the accompanying Xe-131^m was used for detection.

Before labeling, the samples were annealed at the highest experimental temperatures for several hours. The surfaces were thoroughly cleaned and washed in CCl_4.

To avoid charge-build-up during ion bombardment, caused by low electrical conductivity, the samples were mounted on an aluminum plate and masked with aluminum foil which contained a window to allow the beam to enter. Care was taken to hit both sample and foil with the beam and thus get charge compensation through secondary electrons [4]. Both the aluminum plate and foil were grounded.

3.2 Annealing

Annealing was performed in air using a wire-wound tube furnace. Temperatures were read using Pt/Pt-Rh thermocouples. The annealing time in taking F-versus-T curves was always 5 min at each temperature at intervals of 75 to 100 °C. The temperature range was 50 to 600 °C. Some specimens were annealed for 5 min at only one temperature in this range. Other specimens were annealed isothermally at 240, 300 or 400 °C for periods of up to several days.

3.3. Counting

In ion bombardment work usually only one kind of radioactive nuclide is present in the sample situated near to the surface. Thus, counting is favorably done at the bombarded surface of the sample. To this purpose all samples were counted before heating in a flow-type proportional counter. Following each isochronal heating step or at suitable intervals during isothermal annealings the samples were cooled to room temperature and counted again.

[18] F. BROWN, in J. BERGSTRÖM et al., Nucl. Instr. Methods **21**, 249 [1963].

3.4. Range-curves

Range-curves were obtained for xenon and all three concentrations using a chemical dissolution technique. These results are reported elsewhere [16]. Some crystals were bombarded to 4×10^{13} Xe-ions/cm^2 and annealed for 5 min to different temperatures before taking range-curves.

4. Results

4.1. Vaporization

In ion bombardment work, one deals with very short diffusion distances ($\lesssim 10^3$ Å). An interpretation of release data is thus only possible if one determines whether, or how much, vaporization contributes to the gas release. KELLY and MATZKE [4] gave a formula which relates vapor pressure data to a "minimum vaporization temperature (MVT)" which was suitably defined as the temperature at which 5 atom layers evaporate within the experimental annealing time of 5 min. As ranges usually are in the order of about 50 to 200 atom layers, vaporization will not be important below MVT. Using the mentioned formula and vapor pressure data [19] one obtains MVT $\gtrsim 350$ °C. This value gives a lower limit and is probably valid for annealing in vacuum. Ambient gas, however, will reduce the rate of evaporation. Therefore, weight loss data for the atmosphere used (motionless air) were measured using the same crystals as for the diffusion studies. Fig. 3 contains the results. It is seen that in isochronal work with annealing periods of 5 min evaporation can be neglected below about 500 °C.

Recent data of DAWSON, BARR and PITT-PLADDY [20] are in good agreement with the present data, the activation energy for evaporation being the same [(2.2 ± 0.1) eV], the rate of evaporation, however, being slightly slower than in the present study.

4.2. Gas release

Fig. 4 shows the effect of ion energy at a dose of 4×10^{13} Xe-ions/cm^2 on gas release at low temperatures. It is seen that with decreasing energy an increasing percentage of the gas is released at temperatures below $0.5\,T_m \approx 230$ °C (T_m = melting point on the absolute temperature scale). At an energy of 40 keV this release at low temperatures is negligible. At 20, 10, and 5 keV the amount of gas released below 230 °C is approximately proportional to the range of the gas. The release curves for the remaining energies of 2, 1, and 0.5 keV finally are nearly identical.

In Fig. 5 isothermal release curves for pure and doped KBr are shown. The ion energy in these and the following experiments was kept constant at 40 keV to avoid influences of surface proximity. By increasing the ion dose from 4×10^{13} (Xe-133) to 2×10^{16} ions/cm^2 (Xe-131) a retardation of gas release is found for all three materials. Within one set of experiments with the same gas concentration,

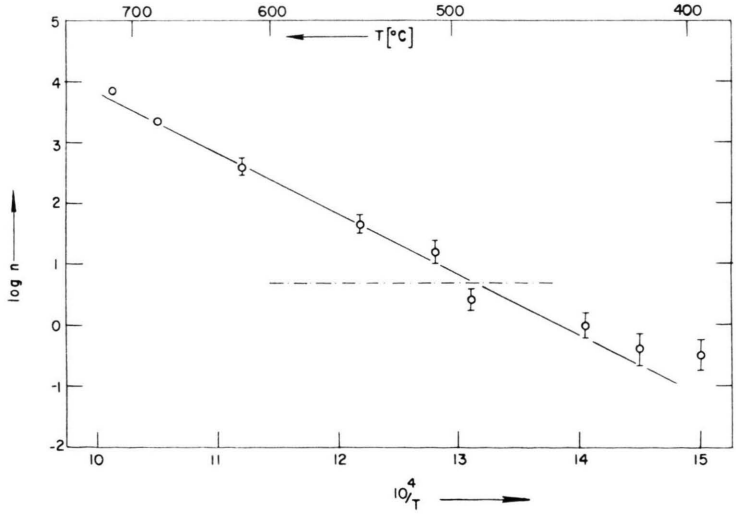

Fig. 3. Weight loss of KBr single crystals due to evaporation during annealing in air. n is the number of atom layers evaporated per 5 min annealing time. It is seen that 5 atom layers/5 min will evaporate at about 490 °C.

[19] B. H. ZIMM and J. E. MAYER, J. Chem. Phys. **12**, 362 [1944].

[20] D. K. DAWSON, L. W. BARR, and R. A. PITT-PLADDY, Brit. J. Appl. Phys. **17**, 657 [1966].

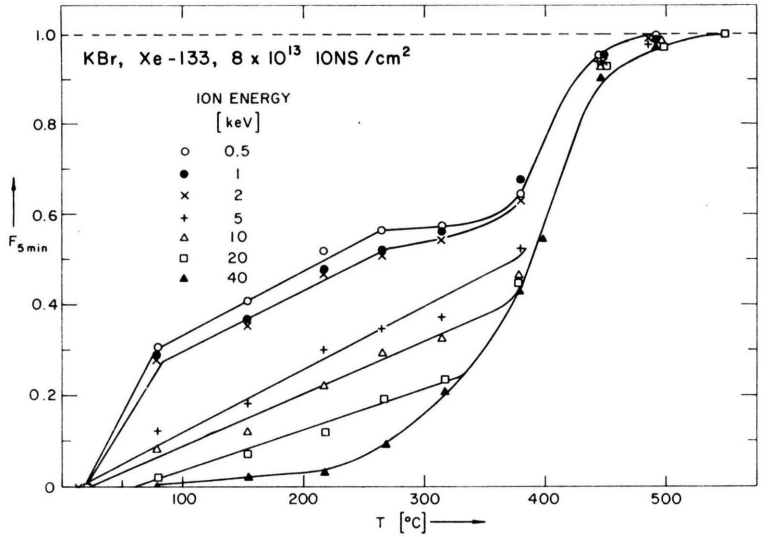

Fig. 4. Isochronal release of Xe-133 from KBr-single crystals following ion bombardment to a dose of 4×10^{13} ions/cm^2. By varying the energy of the incident beam between 0.5 and 40 keV the effect of surface proximity on gas release at low temperatures is shown.

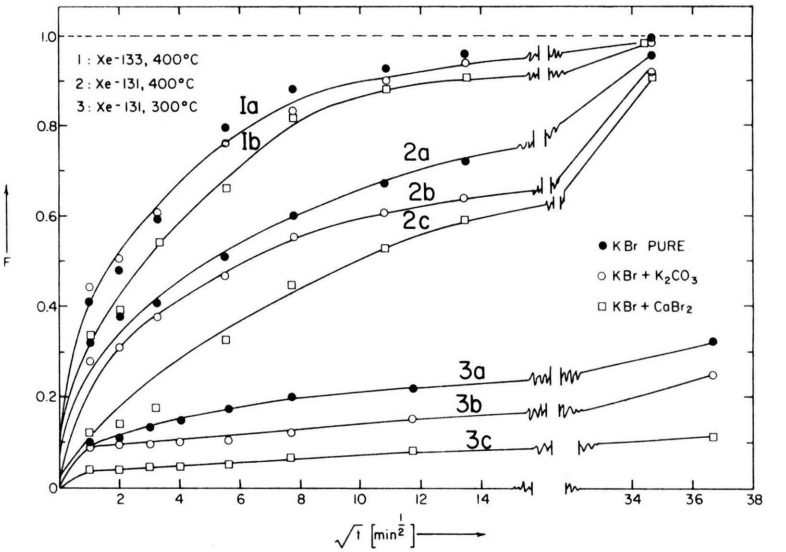

Fig. 5. Isothermal release of Xe-131 (high dose of 2×10^{16} ions/cm^2) and Xe-133 (intermediate dose of 4×10^{13} ions/cm^2) from pure and doped KBr single crystals at 300 and 400 °C.

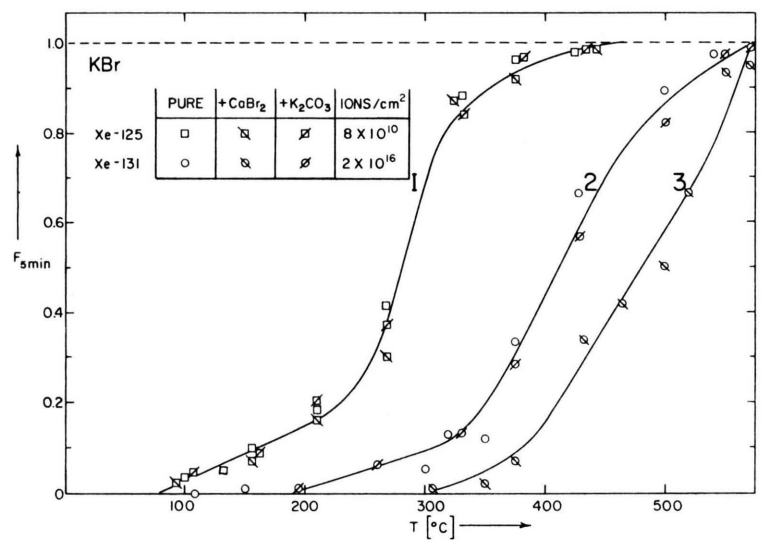

Fig. 6. Isochronal release of Xe-125 (low dose of 8×10^{10} ions/cm^2) and Xe-131 (high dose of 2×10^{16} ions/cm^2) from pure and doped KBr single crystals.

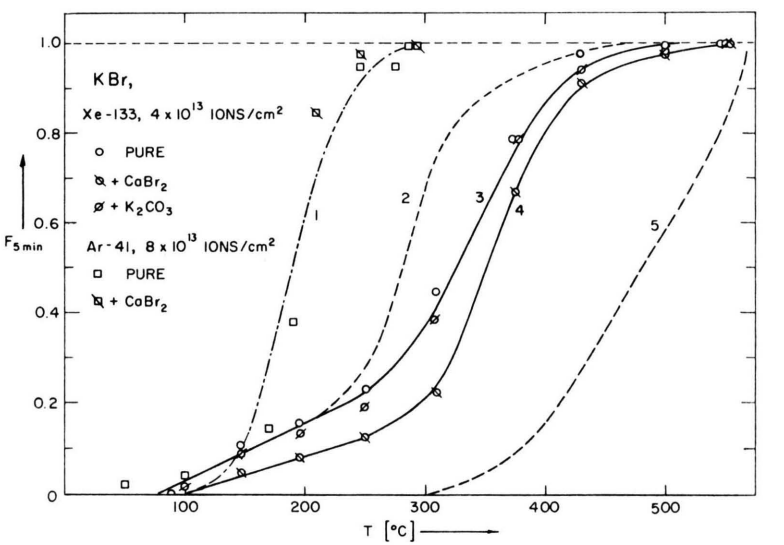

Fig. 7. Isochronal release of Ar-41 (intermediate dose of 8×10^{13} ions /cm^2) and Xe-133 (intermediate dose of 4×10^{13} ions/cm^2) from pure and doped KBr single crystals. Curve 2 represents release following bombardment to a low dose of 8×10^{10} ions/cm^2 and is identical with curve 1 of Fig. 6. Curve 5 shows release following bombardment to a high dose of 2×10^{16} ions/cm^2 and is identical with curve 3 of Fig. 6.

the release from doped KBr is retarded with respect to the release from the pure material. The influence of K_2CO_3 additions is smaller than that of $CaBr_2$ additions though this may reflect only the low solubility of CO_3. The retardation of the gas release in doped KBr is more pronounced at the high dose and especially at small values of time.

The same behaviour is found in isochronal annealings as shown in Figs. 6 and 7. Using a very low gas concentration (8×10^{10} ions/cm^2, Xe-125) no significant effect of dopig is observed. At higher gas concentrations (4×10^{13} or 2×10^{16} Xe-ions/cm^2) release is retarded, i. e. shifted to higher temperatures. The effect is more pronounced in the specimens doped with $CaBr_2$. Little gas release occurred at low temperatures ($<0.4\,T_m$): 10% at the low dose bombardment and 0% at the high dose bombardment.

The release of Ar-41 occurs at much lower temperatures than the release of xenon although an intermediate gas concentration (8×10^{13} Ar-ions/cm^2) was used. The release curve is sigmoidal with an unusually small temperature width. No significant effect of doping is found within the few experiments performed.

Fig. 8 shows distribution curves for Xe-133 (4×10^{13} ions/cm^2) following 5 min anneals to different temperatures. No diffusion has taken place at 115 °C. An increasing penetration is noted at 200, 240, 300, 400 and 500 °C. Only the percentage of the gas which remained in the solid is considered, e. g., the total residual activity of the sample annealed to 500 °C is 4.5%.

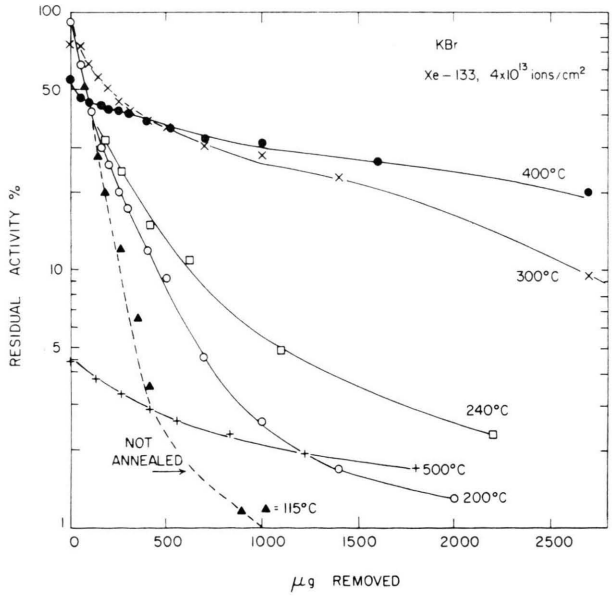

Fig. 8. Depth distribution of Xe-133 (intermediate dose of 4×10^{13} ions/cm^2) in KBr single crystals after annealing for 5 min to different temperatures. The dotted line shows the distribution of Xe-133 prior to annealing.

The release of xenon from layers of KBr evaporated onto glass plates was practically identical to the release from single crystals. In a last series of experiments the diffusion of xenon *through* evaporated layers of KBr was measured. For this purpose, layers of KBr were evaporated onto KBr- or KI-crystals which previously had been bombarded with a low dose of 8×10^{10} Xe-ions/cm^2. Fig. 9 shows that the subsequent release is shifted by about 30 – 50 °C towards higher temperatures compared to the release from normal crystals (drawn lines in Fig. 9).

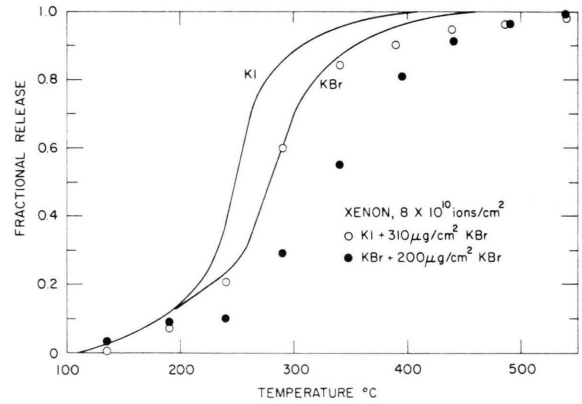

Fig. 9. Release of Xe-125 (low dose of 8×10^{10} ions/cm^2) from KBr or KI (drawn curves) and from KBr- and KI-crystals which were coated with evaporated layers of KBr immediately following bombardment.

5. Discussion

5.1. Gas release at low temperatures

Several authors [3, 9, 12, 21, 22] have shown that gas located near the surface can be released at temperatures below those of normal volume diffusion (stage II) from various substances. Matzke and Whitton [3] proved further that in some cases such a release at temperatures below 0.4 to 0.5 T_m can be correlated to two different experimental conditions: reduction of the sample during the diffusion anneal and to an-

[21] D. P. Corkhill and G. Carter, Phys. Letters **18**, 264 [1965].
[22] A. Auskern, J. Amer. Ceram. Soc. **47**, 390 [1964].

nealing of a bombardment induced structural change. For MgO the data [3] were consistent with an idealized model in which all the gas is released from a surface layer of constant thickness and any gas deeper in the solid is not mobile until the temperatures of volume diffusion are reached. The thickness of this layer was estimated to be roughly 20 ± 10 atom layers.

Similar results were found for KBr in this study. Gas release at low temperatures (stage I) was dominant only at low bombardment energies and thus when the gas was in the proximity of the surface. The combination of high gas concentration and high energy did not lead to release at low temperatures. No indication of a bombardment induced structural change was found by reflection electron diffraction or by electron micrographs of the surface even at the highest dose at high energy (40 keV Xe-131) or at an intermediate dose at low energy (0.5 keV Xe-133). Thus, the release from KBr at low temperatures seems to be related to the proximity of gas to the surface, in possible connection to damage, rather than to damage and its annealing *alone*.

The gas release followed the temperature dependence expected for "damage diffusion" [11] i. e. the release occurred over a much wider temperature range than is compatible with a single ΔH. Such a release process can be approximated by a model involving single jumps of the gas atoms and a spectrum of activation enthalpies with equal weighting between the lower limit, ΔH_1, and the upper limit, ΔH_2. Applying the mathematics given by KELLY [11] and assuming $k_0 = 10^{15 \pm 1}\ \mathrm{sec}^{-1}$ (see refs. [3, 4]), the data of Fig. 4 yield $\Delta H_1 = 23 \pm 5$ kcal/mole and $\Delta H_2 = 42 \pm 5$ kcal/mole.

The amount of gas released below about $0.4\, T_m$ is roughly proportional to the range of the gas. Thus, similar [3] to MgO, all gas released can be approximated as being due to an enhanced release from a surface layer of KBr of constant thickness, and any gas deeper in the solid not being mobile at these low temperatures. It is difficult to give an exact value for this thickness, as the range-energy relation for the system Xe – KBr is not known, the only range curves available being for 40 keV ions [16]. An extrapolation to lower energies is not easy to perform as besides the range also the shape of the distribution profile – and thus the gas concentration in the outermost surface layers – will depend on the incident ion energy. DAVIES and SIMS [23] gave the relative height of the distribution curve at the distance $x = \frac{1}{4} R_p$ from the surface for bombardments of aluminum with Na-24 and K-42. The values decreased from 0.5 at 10 keV to 0.25 at 60 keV. Hence, a relatively small percentage of the gas may be near the surface at the higher energies. Thus, only a rough estimation of the thickness of the surface layer which may contribute to the gas release at low temperatures could be made. A value of 25 ± 10 atom layers was obtained, in approximate agreement with the results deduced [3] for MgO.

No apparent difference was found in the release following bombardment with the three lowest energies used: 2, 1, and 0.5 keV. Furthermore, a fast initial release between ambient temperature and about 60 °C was observed as reported previously [4] for KCl. This is not incompatable with the above explanations. First, one cannot simply extrapolate range data to low energies. This was shown by DOMEIJ et al. [24] for amorphous Al_2O_3: at very low energies of 0.5 to 5 keV, the variation in range was at most a factor of 2 for the energy variation of a factor of 10. Furthermore, at the three low energy bombardments of KBr, the "sticking factor", i. e. the fractional retention of the incident beam, was < 1. Similar results have been reported by BROWN and DAVIES [25] for a variety of metals: The sticking factor approached 1 at energies above about 5 keV and decreased at lower energies to about 0.1 to 0.5 at 1 keV. A low sticking factor may be caused by at least four processes: backscattering, gas-gas sputtering [21], escape by easy diffusion, or chemically altered surface layers (e. g. adsorbed gas, corrosive attack by water vapour etc., deposition of organic materials in the vacuum). The latter two may lead to escape of gas at about ambient temperature during bombardment, may affect the range distribution, and may explain the first initial release from KBr.

5.2. *Volume diffusion (stage II)*

a) Diffusion of xenon: At the lowest dose used, 8×10^{10} ions/cm^2 corresponding to $\approx 10^{-5}$ at % gas concentration, both isothermal and

[23] J. A. DAVIES and G. A. SIMS, Can. J. Chem. **39**, 601 [1961].
[24] B. DOMEIJ, F. BROWN, J. A. DAVIES, and M. MCCARGO, Can. J. Phys. **42**, 1624 [1964].
[25] F. BROWN and J. A. DAVIES, Can. J. Phys. **41**, 844 [1963].

isochronal release curves followed the kinetics for a volume diffusion process. Fig. 3 shows that this release went to completion at about 450 °C. At this temperature, less than 1 atom layer evaporates within the experimental annealing time. Thus, the release curve 1 of Fig. 6 could be evaluated using the mathematics of Section 2.3. The results are shown in Table 3. An activation enthalpy of about 1.4 ± 0.2 eV and a frequency factor $D_0 \approx 10^{1\pm2}$ cm^2

approach	ΔH (eV)		D_0 (cm^2 sec^{-1})	
	Ar	Xe	Ar	Xe
A	1.2 ± 0.2	1.3 ± 0.2	$3 \times 10^{-1\pm1}$	$3 \times 10^{-1\pm1}$
B	1.6 ± 0.2	1.5 ± 0.2	$10^{6\pm2}$	$10^{1\pm2}$
C	1.4 ± 0.2	1.3 ± 0.2	$10^{4\pm1}$	$10^{1\pm1}$
KALBITZER	1.6 ± 0.1	—	2×10^2	—
RICHTER and ZIMEN	1.55	—	1.5×10^5	—

Table 3. Diffusion constants for volume diffusion (stage II) of argon and xenon in KBr.

sec^{-1} seem to be representative for the volume diffusion of xenon in KBr. No obvious effect of doping on xenon release was found. Thus, a diffusion mechanism independent of single vacancies is indicated. This implies that xenon does not diffuse by a vacancy mechanism via single potassium or bromine vacancies. The alternative remains between an interstitial diffusion and diffusion in small vacancy clusters, e. g. in vacancy pairs. The latter mechanism seems to be favoured because of the big size of the xenon atoms. It is of interest that a role for divacancies in particular has been inferred in anion diffusion work on both KBr [26] and KCl [27].

b) Diffusion of argon: Though no low concentration of argon could be employed the release data will be tentatively evaluated using the mathematics for stage II. The diffusion of argon (Fig. 7) occurred at much lower temperatures than the corresponding release of xenon and the release curve was very steep which indicates, according to approaches *B* and *C* of Section 2.3, an abnormally high D_0. Conversely, approach *A* of a fixed, ideal range of D_0's yielded a lower ΔH. As shown in Table 3, a ΔH of 1.5 ± 0.2 eV was obtained using approaches *B* and *C*, similar to that for xenon and in agreement with previous data of KALBITZER [28] and RICHTER and ZIMEN [29]. D_0 was about $10^{5\pm2}$ cm^2 sec^{-1}, again in agreement with the results of RICHTER and ZIMEN. These authors and the present results suggest that doping does not affect argon diffusion. Therefore again, an interstitial diffusion or a mobility via vacancy clusters remains. As the diffusion coefficients for argon were higher by about 2 to 3 orders of magnitude than the diffusion coefficients for xenon, and as the smaller argon atoms can be accommodated into smaller positions, either the interstitial mechanism is favoured for argon diffusion in KBr, or else clusters of constant size are involved (as with xenon) but the clusters are smaller.

While comparing the present data with those obtained following neutron activation [28, 29] one has to consider that the gas concentration in the present ion bombardment work was much higher ($\approx 10^{-2}$ atom-%) than the argon concentration in reactor irradiated samples ($\approx 10^{-10}$ to 10^{-7} atom-%. If the release data are interpreted in terms of trapping then the ratio of the diffusion distance to the spacing of trapping centers is important for the trapping effect and this ratio is comparable for both cases [30]. The observed agreement of the diffusion constants is not surprising in such a case. If, on the other hand, an intrinsic process involving *unassociated* gas atoms governs the release, then the observed agreement of the diffusion constants indicates that gas concentrations up to $\approx 10^{-2}$ atom-% and the accompanying radiation damage do not affect argon diffusion. Contrary results were obtained for xenon diffusion (see Section 5.3) thus given support to the suggestion that the diffusion mechanism for xenon is different from that for argon.

RICHTER and ZIMEN [29] in their work on argon diffusion in reactor irradiated KBr reported a second transport process above 500 °C with an activation enthalpy of only 0.36 eV. No such process could be observed in the present study. Because of the short diffusion distances in the present work, release went to completion before 500 °C were reached.

[26] D. K. DAWSON and L. W. BARR, Proc. Brit Ceram. Soc., in press.
[27] L. W. BARR, J. A. MORRISON, and P. A. SCHROEDER, J. Appl. Phys. **36**, 624 [1965].
[28] S. KALBITZER, Z. Naturforschg. **17 a**, 1071 [1962].
[29] A. H. K. RICHTER and K. E. ZIMEN, Z. Naturforschg. **20 a**, 666 [1965].
[30] R. KELLY, C. JECH, and HJ. MATZKE, to be published.

5.3. *Trapping of xenon and retarded release at high gas concentrations*

Both isothermal and isochronal annealings of samples bombarded to increased doses of 4×10^{13} or 2×10^{16} ions/cm^2 showed a retarded release, i. e., a given F-value was not obtained before longer times or higher temperatures were reached. Such retarded release may be taken as an indication of some sort of trapping. Trapping processes are known from measurements of rare gas diffusion in various substances and have been explained by gas-gas or gas-defect interactions, where the defects may be pre-existing or radiation-induced (e. g. [2, 13, 31]). Increasing the dose from 4×10^{13} to 2×10^{16} Xe-ions/cm^2 increased the retardation of the gas release from KBr (Figs. 5 to 7). At both doses, however, the effect of increased gas concentration was mainly one of temporary retardation rather than of permanent trapping as release went to completion at long enough times or high enough temperatures. In curve 3 of Fig. 7, however, there is indication that evaporation contributed to the release of the last 30% of the gas.

At present, no electron-microscopic examination of neutron irradiated or ion bombarded KBr has been published to reveal possible trapping centers. In addition, alkali halides seem to be unstable in the electron beam of the microscope [32, 33]. However, voids and dislocations loops have been observed in electron bombarded KCl. Thus, these defects might be responsible for the trapping of xenon in KBr.

The retarded release of xenon from KBr was affected by doping. K_2CO_3 additions showed only a little effect, as would be expected because of their small solubility. $CaBr_2$ additions, however, markedly increased the extent of the trapping (Figs. 5 to 7). Doping of KBr with $CaBr_2$ leads to an increased population of cation vacancies which are the more mobile ones, and a decreased population of anion vacancies. This shows that, as with [2] UO_2, the concentration of single vacancies is one of the factors influencing trapping phenomena in KBr.

5.4. *Complementary experiments*

To elucidate further the diffusion mechanism of xenon at intermediate or low gas concentrations, two complementary sets of experiments were performed.

At an intermediate dose of 4×10^{13} ions/cm^2 and different temperatures, distribution profiles were measured following diffusion (Fig. 8). No appropriate solution of the diffusion equation exists at present to evaluate these curves as at this dose gas is *weakly* trapped, even [34] at $t=0$. However, the curves of Fig. 8 prove that there is a fairly random mobility of this trapped gas and confirm that this release is not an artifact due to evaporation.

It is still not clear yet whether the data obtained following low dose bombardment are applicable to truly undamaged material or whether the suggested mobility of xenon in small vacancy clusters (e. g. vacancy pairs) is a special kind of a trapping effect for low levels of radiation damage. Therefore, the diffusion of xenon at a low dose of 8×10 ions/cm^2 through *unbombarded* layers of KBr was measured in a second set of experiments (Fig. 9). It was mentioned in Section 4.2, that evaporated layers of KBr, when ion bombarded, show a gas release identical to that from bombarded single crystals. In addition, the layers recrystallized during heating. Evaluation of the data of Fig. 9 yields approximately the same diffusion coefficients as those obtained from Fig. 6, curve 1, i. e., single crystals bombarded to a low dose. This is in favour of the low dose release data being typical for the limiting case of undamaged material with no gas-gas or gas-damage interaction occurring.

Two topics have been bypassed in the above discussion. These are the influence of an increased concentration of impurities at the surface and thus the occurrance of a space charge layer [35, 36], and the possibility of dissolved oxygen in surface near regions [26]. The reason is that any influences of these effects are considered to be small: The space charge layer in the doped crystals is not likely to affect the rare gas mobility because the rare gases are probably present as neutral atoms. Any increased concentration of impurities near the surface will exaggerate

[31] R. Kelly and E. Ruedl, Phys. Stat. Sol. **13**, 55 [1966].
[32] Y. Kawamata and T. Hibi, J. Phys. Soc. Japan **20**, 242 [1965].
[33] G. Honjo and K. Yagi, J. Phys. Soc. Japan, Suppl. III, **18**, 355 [1963].
[34] Hj. Matzke, to be published.
[35] K. Lehavec, J. Chem. Phys. **21**, 1123 [1953].
[36] A. Allnat, Amer. J. Phys. Chem. **68**, 1763 [1964].

the effect of impurities on rare-gas diffusion and trapping following ion bombardment and thus not affect the above conclusions. The solubility of oxygen, finally, does not occur before an incubation period which is longer than the heating time used in this study and furthermore, the oxygen solubility is probably not important at temperatures below 500 °C, i. e., it should not appreciably affect the results of this study. In addition, dissolved oxygen should compensate the effect of $CaBr_2$-addition. However, an effect of these additions was found.

6. Summary

The diffusion of argon and the diffusion and trapping of xenon in ion bombarded single crystals of KBr with varying vacancy concentration has been studied.

The results of argon diffusion between 20 and 300 °C are compatable with an interstitial diffusion mechanism largely independent of both vacancy and gas concentration, but mobility via small vacancy clusters of constant size cannot be excluded. The diffusion process can be described by an activation enthalpy of 1.5 ± 0.2 eV, in agreement with results by KALBITZER and RICHTER and ZIMEN, and a frequency factoı D_0 of about $10^{5\pm2}$ cm^2 sec^{-1}, again in agreement with RICHTER and ZIMEN's value.

The diffusion of xenon was much slower than that of argon, as observed before for [4] KCl and CaF_2. In the limiting case of low gas concentration, no significant effect of vacancy concentration on release was observed. This release yielded an activation enthalpy of 1.4 ± 0.2 eV and a D_0 of $10^{1\pm2}$ cm^2 sec^{-1}. The data are consistant either with an interstitial diffusion mechanism or, preferably, with xenon being mobile in small vacancy clusters of constant size, e. g. vacancy pairs, even in unbombarded KBr.

At increased xenon dose, a retardation of the gas release (temporary or weak trapping) was observed. This retardation was more pronounced in doped crystals, thus giving evidence that the vacancy concentration is one of the factors governing trapping phenomena.

A fast gas release at abnormally low temperatures was observed if much of the gas was near to the surface. This release could be approximated with a spectrum of activation enthalpies having limits of $\Delta H_1 = 1.0 \pm 0.2$ eV and $\Delta H_2 = 1.8 \pm 0.2$ eV.

Acknowledgements

The generous help of the staff of the Chemistry and Metallurgy Division at the Chalk River Nuclear Laboratories is gratefully acknowledged. The KBr single crystals were kindly supplied by Dr. J. ROLFE, NRC, Ottawa. The National Research Council, Ottawa, provided a Post Doctoral Fellowship, in the course of which this work was carried out.